Elżbieta Hędrzak (ehedrzak@indy.chemia.pk.edu.pl)
Piotr Michorczyk

Institute of Organic Chemistry and Technology, Faculty of Chemical Engineering and Technology, Cracow University of Technology

The application of 3d printing in the designing of channel structures in monolithic catalysts dedicated to the oxidative coupling of methane

Zastosowanie drukowania 3d do modelowania struktury kanałów w monolitycznych katalizatorach dedykowanych dla procesu utleniającego sprzęgania metanu

Abstract

In this work, a new preparation method is proposed to obtain high temperature monolithic structures for catalytic applications. A commercial 3D printer was used to synthesise polymeric templates that were utilised in the designing of channel structures in monolithic catalysts. New materials with manganese and sodium tungstate supported on corundum with macropores of well-defined shapes and sizes were prepared; their catalytic performance was investigated in the process of the oxidative coupling of methane.

Keywords: monolithic catalysts, 3D printing, oxidative coupling of methane

Streszczenie

W niniejszym artykule zaproponowano nową metodę otrzymywania wysokotemperaturowych struktur monolitycznych do zastosowań katalitycznych. Wykorzystano komercyjną drukarkę 3D, aby zsyntezować polimerowe templaty, których użyto do modelowania struktury kanałów w monolitycznych katalizatorach. Przygotowano nowe materiały zawierające mangan i wolframian sodowy na nośniku korundowym, posiadające makropory o dobrze zdefiniowanym kształcie i rozmiarze. Ich właściwości katalityczne zostały zbadane w procesie utleniającego sprzęgania metanu.

Słowa kluczowe: katalizatory monolityczne, drukowanie 3D, utleniające sprzęganie metanu

1. Introduction

Currently, natural gas is under-utilised as there are no feasible ways to convert large amounts of methane, the main component of natural gas, into products that are of any value. The oxidative coupling of methane (OCM) is a promising route for the production of ethane or ethene. Ethylene is a vital building block in the chemical industry which has seen, as expected, an increasingly high demand over the last few years. Feedstock such as naphtha or ethane, from which ethylene is produced using the cracking process, is beginning to run out; therefore, the OCM process is worthy of investigation. Thus far, no economically viable process has been put into practice despite many attempts to do so; the reason for this is the lack of active, selective and, in particular, stable catalysts [1, 2].

A large number of catalyst systems have been studied extensively. Sodium-tungsten-manganese-supported-silica catalyst (with commonly used composition of 2wt.% of Mn and 5wt.% of Na_2WO_4) is one of the most active catalysts that shows good performance and stability over a long period on stream in the OCM process with up to 30% methane conversion and 80% selectivity to ethane and ethene. However, the obtained yield and stability still need to be improved for industrial applications [1–6].

Apart from conventional particle catalysts, some monolithic catalysts were tested in the OCM process, e.g. Na_2WO_4-Mn/SiC (foam) [7], Mn-Na_2WO_4/SiO_2,Al_2O_3/FeCrAl (alloy foil) [8], Na_3PO_4-Mn/SiO_2/cordierite (two-stage catalyst bed reactor with Na_2WO_4-Mn/SiO_2 particle catalyst) [9], Ce-Na_2WO_4-Mn/SBA-15/Al_2O_3/FeCrAl (dual-bed reactor with Na_2WO_4-Mn/SiO_2 particle catalyst) [10] – all of these exhibited a strong level of performance [7–10]. Recently, Mn- and Na_2WO_4-containing ceramic monoliths, which were obtained on the basis of 3D printed polymeric templates, were tested by our research group. These catalysts exhibited excellent performance in the OCM process [11].

In this work, monolithic catalysts with manganese and sodium tungstate supported on corundum with macropores (channels) with well-defined shapes and sizes were prepared. In order to obtain high temperature monoliths, a novel preparation method was proposed. This method involved the use of a commercial 3D printer to synthesise polymeric templates for catalysts. Five catalysts were prepared – these differed from each other in the way in which their active components were added or in the type of macropores. Their catalytic performance was investigated in the process of oxidative coupling of methane.

2. Experimental

2.1. Catalysts preparation

Two digital models of matrixes were designed using the SketchUp software program and printer software – these models are presented in Fig. 1. Subsequently, the models were converted into STL files and mathematically sliced into 25 μm layers by the printer software. The matrixes were than printed using a digital light processing method with a resolution

of 30 μm and acrylic resin. After printing, they were washed with acetone and cured under UV lamp for six hours. Full details of the 3D printing procedures and a description of the currently applied techniques have been previously described by the authors in mini-reviews [12, 13]. The hardened polymeric matrixes were used as hard templates for the preparation of monolithic catalysts.

Reagents used for the synthesis were: corundum (alumina oxide powder, Microgrit WCA, size 15 μm); commercial solution of sodium water glass (sodium silicate, *CAZET* Kampinos); sodium tungstate dihydrate (pure p.a., >99%, Polish Chemical Reagents, size 100 μm); manganese (II) nitrate tetrahydrate (pure p.a., Chempur); ethyl alcohol (96% pure, POCH).

Five monolithic catalysts with manganese and sodium tungstate supported on corundum were prepared. The concentrations of solutions and mixtures were selected in order to obtain the catalysts containing 2wt.% of Mn and 5wt.% of Na_2WO_4 relative to the weight of α-Al_2O_3. The catalysts differed in the type of the template used and/or the way in which the active components were added. The steps involved in the preparation of the catalysts are described in Table 1 and presented in Figs. 2 and 3. The synthesis of the catalysts consisted of 4–7 steps. These steps were: pre-impregnation with heating; filling template with mixture of support or catalyst precursor; drying; calcination; impregnations followed by calcinations. The monolithic structures were obtained in the process of the calcination in air, during which the templates were burnt.

2.2. Catalytic performance

The catalytic tests were carried out in a continuous flow quartz reactor. The reactor was 16 mm in external diameter, 300 mm in length and had a wall thickness of 1 mm. The weight of the catalyst sample was 4.5 g each time. Before the process, the catalyst placed in the reactor was heated in helium (99.99% purity, Linde) for 30 minutes at 780°C. During the process, the reactor was fed with a mixture of methane (99.95% purity, Linde), oxygen (99.5% purity, Linde) and helium. After 20 minutes on stream, the first data point (i.e. the instantaneous composition of the reaction gas) was measured. The reaction mixture was composed on-line with Bronkhorst volumetric flow regulators. The temperature that was measured with a thermocouple was the central temperature of the tube furnace in the middle of which the catalyst was placed. The influence of process parameters such as temperature, methane to oxygen molar ratio and complete substrate volumetric flow rate (or gas hourly space velocity) was studied for three catalysts – IMs, MMs and IIs. Additionally, the influence of temperature was examined for 0Ms and IIt catalysts.

The composition of the mixture after the process was analysed on-line using the Agilent 6890N gas chromatograph equipped with two columns (molecular sieve 5A for the analysis of CO and O_2 and Hayesep Q for the analysis of H_2, CO_2, H_2O and hydrocarbons) and thermal conductivity detectors. Conversion of methane $\left(\alpha_{CH_4}\right)$, selectivity to ethane and ethene $\left(S_{C_2}\right)$, and selectivity to propane and propene $\left(S_{C_3}\right)$ were calculated as described below. The carbon mass balance was always better than 90%.

Table 1. Steps of 2%Mn-5%Na$_2$WO$_4$/Al$_2$O$_3$ catalyst preparation. Designation: first letter – the way of introducing Mn; second letter – the way of introducing Na$_2$WO$_4$; third letter – the type of grid holes (0 – the lack of a component, M – in mass, I – impregnated, s – square, t – triangle)

Catalyst designation	Step 1 Pre-impregnation with heating	Step 2 Filling template with mixture of support/catalyst precursor	Step 3 Drying	Step 4 Calcination	Step 5 Impregnation I	Step 6 Calcination	Step 7 Impregnation II	Step 8 Calcination
0Ms	–	Al$_2$O$_3$ + Na$_4$SiO$_4$ sol. + Na$_2$WO$_4$·2H$_2$O = 1:0.5: 0.056 (wt.)	20°C 24 h and 120°C 4h (rate 2°C/min)	850°C 2h (rate 2.7°C/min)	–	–	–	–
IMs	–				ethanol sol. of Mn(NO$_3$)$_2$·4H$_2$O Al$_2$O$_3$:Mn = 1:0.02 (wt.)	850°C 2h (rate 2.7°C/min)	–	–
MMs	Al$_2$O$_3$ + ethanol sol. of Mn(NO$_3$)$_2$·4H$_2$O Al$_2$O$_3$:Mn = 1:0.02 (wt.) 250°C 100 min	Mn/Al$_2$O$_3$ + Na$_4$SiO$_4$ sol. + Na$_2$WO$_4$·2H$_2$O = 1.032: 0.5:0.056 (wt.)			–			
IIs	–	Al$_2$O$_3$ + Na$_4$SiO$_4$ sol. = 1:0.5 (wt.)			aqueous sol. of Na$_2$WO$_4$·2H$_2$O Al$_2$O$_3$: Na$_2$WO$_4$ = 1:0.05 (wt.)	850°C 2h (rate 2.7°C/min)	ethanol sol. of Mn(NO$_3$)$_2$·4H$_2$O Al$_2$O$_3$:Mn = 1:0.02 (wt.)	850°C 2h (rate 2.7°C/min)
IIt								

$$\alpha_{CH_4} = \frac{\sum a_i n_i}{\sum a_i n_i + \alpha_{CH_4} \cdot n_{CH_4}} \cdot 100\%$$

$$S_{C_2} = \frac{(a_{C_2 H_6} \cdot n_{C_2 H_6} + a_{C_2 H_4} \cdot n_{C_2 H_4})}{\sum a_i n_i} \cdot 100\%$$

$$S_{C_3} = \frac{(a_{C_3 H_8} \cdot n_{C_3 H_8} + a_{C_3 H_6} \cdot n_{C_3 H_6})}{\sum a_i n_i} \cdot 100\%$$

where:

n_i – the number of products moles in outlet;
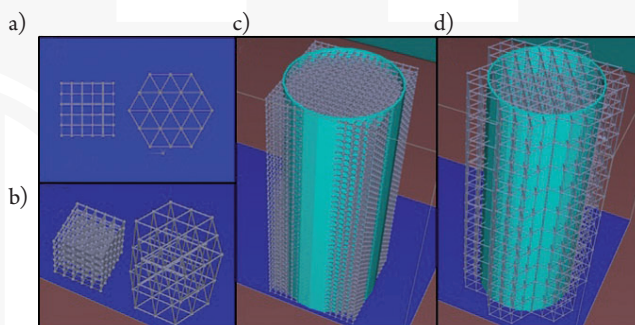
a_i – the number of carbon atoms in 'i' product.

Fig. 1. Design of the templates (view from the printer software): building units (a–b); model giving square type grid holes (c); model giving triangular type grid holes (d)
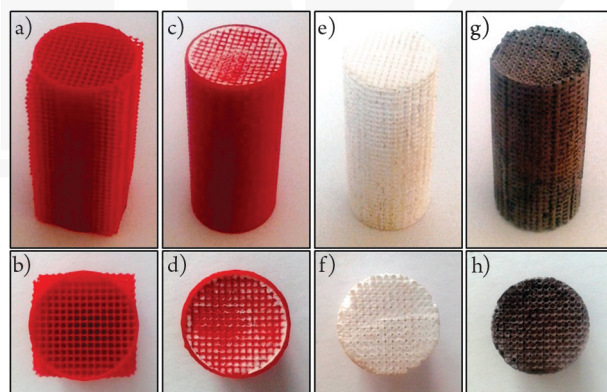
Fig. 2. Monolithic catalyst preparation: printed polymeric template with square type grid holes (a–b); template filled with support precursor (c–d); monolithic support after calcination (e–f); monolithic Mn-Na$_2$WO$_4$/Al$_2$O$_3$ catalyst after double impregnation (g–h). Dimensions: template – 40 mm in height; 16 mm in external and 15 mm in internal diameter; rods forming spatial structure of template – 0.27 mm thick; grid holes – 0.72 mm length of square side; catalyst (after tooling) – 32 mm in height; 15 mm in external diameter; catalyst pores – 0.25 mm in diameter
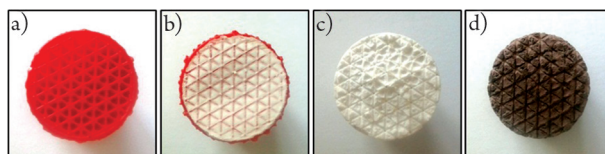
Fig. 3. Monolithic catalyst preparation: printed polymeric template with triangular type grid holes (a); template filled with support precursor (b); monolithic support after calcination (c); monolithic $Mn-Na_2WO_4/Al_2O_3$ catalyst after double impregnation (d). Dimensions: as objects in Fig. 2, except for grid holes – 1.20 mm height of triangle

3. Results and discussion

Table 2 as well as Figs. 4 and 5 summarise the catalytic results obtained over prepared catalysts in the process of the oxidative coupling of methane.

Table 2. Variation of methane conversion, selectivity to C_2, selectivity to C_3 hydrocarbons, ethene to ethane molar ratio with GHSV and methane to oxygen molar ratio at 780°C

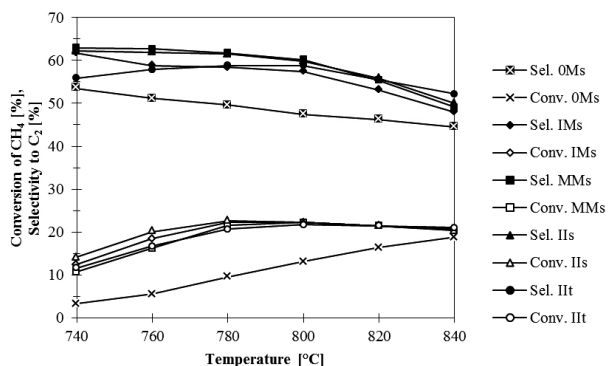| Catalyst	GHSV $[cm^3 \cdot g_{cat}^{-1} \cdot h^{-1}]$	Feed gas $CH_4:O_2:He$ [mol:mol:mol]	Conversion of CH_4 [%]	Selectivity to C_2 [%]	$C_2H_4:C_2H_6$ molar ratio	Selectivity to C_3 [%]
IMs	2067	2:1:2.1	29.9	43.2	2.3	1.6
		3.75:1:4.8	22.3	56.5	2.1	2.0
		7:1:9.85	12.8	70.8	1.3	1.7
	4133	2:1:2.1	18.6	54.0	1.4	1.3
		3.75:1:4.8	7.8	69.8	0.5	0.0
		7:1:9.85	5.1	77.0	0.4	0.0
	6200	3.75:1:4.8	4.2	62.3	0.3	0.0
MMs	2067	2:1:2.1	32.0	33.9	2.2	1.0
		3.75:1:4.8	21.6	60.0	2.0	1.7
		7:1:9.85	13.0	72.3	1.2	1.6
	4133	2:1:2.1	20.3	50.5	1.7	1.2
		3.75:1:4.8	8.6	71.7	0.7	0.0
		7:1:9.85	5.3	79.6	0.4	0.0
	6200	3.75:1:4.8	4.2	74.5	0.3	0.0
IIs	2067	2:1:2.1	35.0	36.6	2.3	1.2
		3.75:1:4.8	22.7	59.6	2.0	1.9
		7:1:9.85	13.6	71.2	1.3	1.5
	4133	2:1:2.1	22.7	50.3	1.8	1.3
		3.75:1:4.8	10.2	70.8	0.7	0.0
		7:1:9.85	5.8	76.4	0.4	0.0
	6200	3.75:1:4.8	4.9	71.9	0.3	0.0

Fig. 4. Variation of methane conversion and selectivity to C_2 hydrocarbons versus temperature. Process conditions: molar ratio of $CH_4:O_2:He = 3.75:1:4.8$, GHSV = 2067 $cm^3 \cdot g_{cat}^{-1} \cdot h^{-1}$
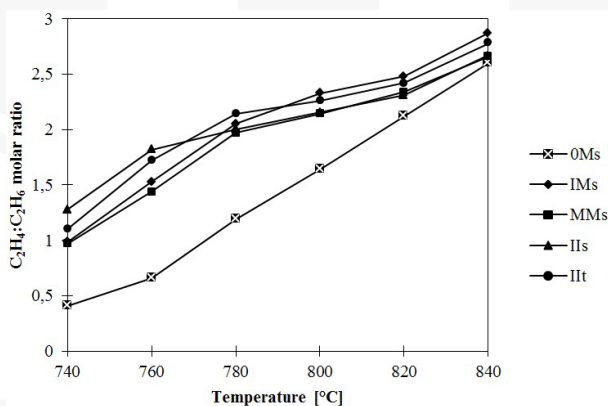

Fig. 5. Variation of ethene to ethane molar ratio versus temperature. Process conditions: molar ratio of $CH_4:O_2:He = 3.75:1:4.8$, GHSV = 2067 $cm^3 \cdot g_{cat}^{-1} \cdot h^{-1}$

With increasing methane to oxygen molar ratio and GHSV (or total volumetric flow rate), methane conversion and ethene to ethane molar ratio decreased, and selectivity to C_2 hydrocarbons increased for three catalysts: IMs, MMs and IIs.

When temperature increased, methane conversion increased and remained almost constant between 780°C and 840°C for all the catalysts expect for 0Ms, for which the conversion increased across the entire studied temperature range. Selectivity to C_2 hydrocarbons decreased for catalysts 0Ms, IMs, MMs and IIs with increasing temperature. For the IIt catalyst, selectivity to C_2 hydrocarbons slightly increased to 780°C and then decreased. For all the catalysts, ethene to ethane molar ratio increased with increasing temperature. The results obtained when using the 0Ms catalyst were noticeably worse than those obtained when using all the others with the exception of results relating to very high temperatures. When the monolith of pure support was used, the results were the worst (4.5% methane conversion, 35.0% selectivity to C_2 and 0.7 ethene to ethane molar ratio at 780°C).

The stability of the $Mn-Na_2WO_4$ monolith with the same composition as the IIs catalyst, which was synthesised in a similar way, was investigated in the OCM process (T = 820°C; GHSV = 2200 $cm^3 \cdot g_{cat}^{-1} \cdot h^{-1}$; $CH_4:O_2:He = 3.8:1.5:4.2$). For a period of 20 hours on stream, the

conversion of methane, yield and selectivity to C_2 remained constant. Therefore, Mn-Na$_2$WO$_4$ catalysts which are described in this work would exhibit good catalytic stability [11].

Comparing the results obtained in the current study with the results obtained by other groups of scientists who investigated the thus far best known conventional Mn-Na$_2$WO$_4$/SiO$_2$ catalyst, it can be observed that the first are slightly inferior. Over the best IIs monolithic catalyst, 22.7% methane conversion and 59.6% selectivity to C_2 hydrocarbons were obtained (T = 780°C; molar ratio of CH$_4$:O$_2$:He = 3.75:1:4.8; GHSV = 2067 cm$^3 \cdot$g$_{cat}^{-1} \cdot$h^{-1}). Over the best particle catalysts supported on silica, 20–30% methane conversion and 70–80% selectivity to C_2 hydrocarbons were achieved [14]. General variations of methane conversion and selectivity to C_2 hydrocarbons obtained in this work are in accordance with literature, e.g. the increase of selectivity to C_2 is usually accompanied by the decrease of methane conversion [14–18]. The increase of CH$_4$ conversion is due to the fact that at higher temperatures, more methane molecules have sufficient energy to reduce the activation energy in the presence of the catalyst (reaching the maximum at about 800°C in the case of Mn-Na$_2$WO$_4$ catalysts); at lower CH$_4$:O$_2$ molar ratios, more oxygen is available for the reaction and at lower helium dilution of the reaction gas (lower GHSV), the contact time with the catalyst is longer. The decrease of C_2 selectivity is a consequence of undesirable oxidation reactions – total oxidation of CH$_4$ and further oxidation of C_{2+} hydrocarbons; these reactions are favoured by high temperature, high oxygen content in the feed and long contact time with the catalyst. The increase of the C_2H_4:C_2H_6 ratio is caused by an increase in the importance of the consecutive oxidative and non-oxidative dehydrogenation reactions of ethane (both catalytic and thermal) at high temperature and high oxygen content, and for long contact times [14, 19–22]. It has also been confirmed that the addition of manganese to the catalysts is necessary to obtain better results [3].

It is very likely that the results can be improved by optimising the process conditions and the structural properties of the catalysts (e.g. size and shape of channels).

The method used to add the active components had little influence on methane conversion, selectivity to C_2 hydrocarbons and ethene to ethane molar ratio for Mn-Na$_2$WO$_4$/Al$_2$O$_3$ catalysts in the same process conditions. Slightly better C_2 yields were reached using the catalyst obtained by the double impregnation method compared to the other two catalysts. The differences in the results were probably connected with the concentration of the active components on the surface of the investigated catalysts. In the case of the samples prepared by the double impregnation method, the concentration of the active compounds was higher than in the case of the monoliths in which these components were incorporated into mass (bulk). Higher surface concentration may be responsible for slightly higher activity at the beginning of the process but can also result in the loss of catalyst activity later, e.g. due to loss of metal oxides after long-term exposure under OCM conditions. This is in line with the results obtained for the conventional catalysts – the catalyst activity values for different preparation methods were comparable but the catalyst prepared by mixture slurry method had better stability than those prepared by impregnation method [1, 18].

In this study, the type of catalyst macropores had very little influence on selectivity to C_2 hydrocarbons, methane conversion and ethene to ethane molar ratio in the same process

conditions. It was expected that the type of macropores would yield more differing results; however, due to the fact that reactions largely occurred not only in the internal pores but on the external walls of the monolith with a relatively large surface – it is difficult to determine whether type of catalyst channels will affect catalyst performance.

4. Conclusions

The monolithic catalysts obtained by using acrylic templates from 3D printing are fairly active and selective in the process of the oxidative coupling of methane to ethylene and ethane. The method of the incorporation of active components into the monoliths did not significantly affect the catalytic performance. Over the prepared $Mn-Na_2WO_4/Al_2O_3$ catalysts (in the conditions: T = 780°C; molar ratio of $CH_4:O_2:He$ = 3.75:1:4.8; GHSV = 2067 $cm^3 \cdot g_{cat}^{-1} \cdot h^{-1}$), selectivity to hydrocarbon products – ethane, ethene, propane and propene, and methane conversion varied in narrow ranges – 58–62% and 21–23%, respectively.

The obtained results suggest that monolithic catalysts can be a good alternative for the conventional catalysts in the OCM process. The new method of the preparation of monolithic catalysts with the use of a 3D printer will be very useful in carrying out more advanced studies in this field.

References

[1] Chua Y.T., Mohamed A.R., Bhatia S., *Oxidative coupling of methane for the production of ethylene over sodium-tungsten-manganese-supported-silica catalyst (Na-W-Mn/SiO$_2$)*, Applied Catalysis A: General, vol. 343, 2008, 142–148.

[2] Arndt S., Otremba T., Simon U., Yildiz M., Schubert H., Schomäcker R., *Mn-Na$_2$WO$_4$/ SiO$_2$ as catalyst for the oxidative coupling of methane. What is really known?*, Applied Catalysis A: General, vol. 425–426, 2012, 53–61.

[3] Elkins T.W., Hagelin-Weaver H.E., *Characterization of Mn-Na$_2$WO$_4$/SiO$_2$ and Mn-Na$_2$WO$_4$/MgO catalysts for the oxidative coupling of methane*, Applied Catalysis A: General, vol. 497, 2015, 96–106.

[4] Michorczyk B., Suszyński K., Smoleń P., Hędrzak E., *Utleniające sprzęganie metanu zintegrowane w jednym reaktorze z odwodornieniem etanu do etenu*, Przemysł Chemiczny, vol. 95, 2016, 1936–1940.

[5] Michorczyk B., Ogonowski J., Michorczyk P., Węgrzyniak A., *Katalizatory dla procesu utleniającego sprzęgania metanu*, Przemysł Chemiczny, vol. 93, 2014, 1166–1173.

[6] Michorczyk B., Hędrzak E., *Study of oxidative coupling of methane integrated with CO oxidation*, Technical Transactions, 2017 (article accepted for publication).

[7] Liu H., Yang D., Gao R., Chen L., Zhang S., Wang X., *A novel Na$_2$WO$_4$-Mn/SiC monolithic foam catalyst with improved thermal properties for the oxidative coupling of methane*, Catalysis Communications, vol. 9, 2008, 1302–1306.

[8] Greish A.A., Glukhov L.M., Finashina E.D., Kustov L.M., Sung J.S., Choo K.Y., Kim T.H., *Comparison of activities of bulk and monolith Mn-Na$_2$WO$_4$/SiO$_2$ catalysts in oxidative coupling of methane*, Mendeleev Communications, vol. 19, 2009, 337–339.

[9] Wang W., Ji S., Pan D., Li C., *A novel particle/monolithic two-stage catalyst bed reactor and their catalytic performance for oxidative coupling of methane*, Fuel Processing Technology, vol. 92, 2011, 541–546.

[10] Wang W., Zhang Z., Ji S., *Particle/metal-based monolithic catalysts dual-bed reactor with beds-interspace supplementary oxygen: Construction and performance for oxidative coupling of methane*, Journal of Natural Gas Chemistry, vol. 21, 2012, 400–406.

[11] Michorczyk P., Hędrzak E., Węgrzyniak A., *Preparation of monolithic catalysts using 3D printed templates for oxidative coupling of methane*, Journal of Materials Chemistry A, vol. 4, 2016, 18753–18756.

[12] Hędrzak E., Michorczyk P., *Trójwymiarowe drukowanie: od projektu do gotowego produktu*, [in:] Leśny J., Panfil M., Nyćkowiak J. (Eds.), *Badania i Rozwój Młodych Naukowców w Polsce. Nauki Techniczne i Inżynieryjne. Część V*, Młodzi Naukowcy, Poznań 2016, 65–71.

[13] Hędrzak E., Michorczyk P., *Trójwymiarowe drukowanie: przegląd metod*, [in:] Leśny J., Panfil M., Nyćkowiak J. (Eds.), *Badania i Rozwój Młodych Naukowców w Polsce. Nauki Techniczne i Inżynieryjne. Część V*, Młodzi Naukowcy, Poznań 2016, 72–78.

[14] Godini H.R., Gili A., Görke O., Arndt S., Simon U., Thomas A., Schomäcker R., Wozny G., *Sol-gel method for synthesis of Mn-Na$_2$WO$_4$/SiO$_2$ catalyst for methane oxidative coupling*, Catalysis Today, vol. 236, 2014, 12–22.

[15] Pak S., Qiu P., Lunsford J.H., *Elementary reactions in the oxidative coupling of methane over Mn/Na$_2$WO$_4$/SiO$_2$ and Mn/Na$_2$WO$_4$/MgO catalysts*, Journal of Catalysis, vol. 179, 1998, 222–230.

[16] Liu H., Wang X., Yang D., Gao R., Wang Z., Yang J., *Scale up and stability test for oxidative coupling of methane over Na$_2$WO$_4$-Mn/SiO$_2$ catalyst in a 200 ml fixed-bed reactor*, Journal of Natural Gas Chemistry, vol. 17, 2008, 59–63.

[17] Shahri S.M.K., Pour A.N., *Ce-promoted Mn/Na$_2$WO$_4$/SiO$_2$ catalyst for oxidative coupling of methane at atmospheric pressure*, Journal of Natural Gas Chemistry, vol. 19, 2010, 47–53.

[18] Wang J., Chou L., Zhang B., Song H., Zhao J., Yang J., Li S., *Comparative study on oxidation of methane to ethane and ethylene over Na$_2$WO$_4$-Mn/SiO$_2$ catalysts prepared by different methods*, Journal of Molecular Catalysis A: Chemical, vol. 245, 2006, 272–277.

[19] Tiemersma T.P., Tuinier M.J., Gallucci F., Kuipers J.A.M., van Sint Annaland M., *A kinetics study for the oxidative coupling of methane on a Mn/Na$_2$WO$_4$/SiO$_2$ catalyst*, Applied Catalysis A: General, vol. 433–434, 2012, 96–108.

[20] Koirala R., Büchel R., Pratsinis S.E., Baiker A., *Oxidative coupling of methane on flame-made Mn-Na$_2$WO$_4$/SiO$_2$: Influence of catalyst composition and reaction conditions*, Applied Catalysis A: General, vol. 484, 2014, 97–107.

[21] Daneshpayeh M., Khodadadi A., Mostoufi N., Mortazavi Y., Sotudeh-Gharebagh R., Talebizadeh A., *Kinetic modeling of oxidative coupling of methane over Mn/Na$_2$WO$_4$/SiO$_2$ catalyst*, Fuel Processing Technology, vol. 90, 2009, 403–410.

[22] Shahri S.M.K., Alavi S.M., *Kinetic studies of the oxidative coupling of methane over the Mn/Na$_2$WO$_4$/SiO$_2$ catalyst*, Journal of Natural Gas Chemistry, vol. 18, 2009, 25–34.